Biophysical Chemistry 141 (2009) 21–28

Contents lists available at ScienceDirect

Biophysical Chemistry

journal homepage: http://www.elsevier.com/locate/biophyschem

The effect of additional disulfide bonds on the stability and folding of ribonuclease A

Pascal Pecher, Ulrich Arnold *

Martin-Luther University Halle-Wittenberg, Institute of Biochemistry and Biotechnology, Kurt-Mothes Str. 3, 06120 Halle, Germany

ARTICLE INFO

Article history:
Received 29 September 2008
Received in revised form 11 December 2008
Accepted 13 December 2008
Available online 30 December 2008

Keywords:
Ribonuclease A
Thermodynamic stability
Protein folding
Disulfide bond
Protein engineering

ABSTRACT

The significant contribution of disulfide bonds to the conformational stability of proteins is generally considered to result from an entropic destabilization of the unfolded state causing a faster escape of the molecules to the native state. However, the introduction of extra disulfide bonds into proteins as a general approach to protein stabilization yields rather inconsistent results. By modeling studies, we selected positions to introduce additional disulfide bonds into ribonuclease A at regions that had proven to be crucial for the initiation of the folding or unfolding process, respectively. However, only two out of the six variants proved to be more stable than unmodified ribonuclease A. The comparison of the thermodynamic and kinetic data disclosed a more pronounced effect on the unfolding reaction for all variants regardless of the position of the extra disulfide bond. Native-state proteolysis indicated a perturbation of the native state of the destabilized variants that obviously counterbalances the stability gain by the extra disulfide bond.

© 2008 Elsevier B.V. All rights reserved.

1. Introduction

The folding process of proteins starts with a hydrophobic collapse or other local events at so-called 'nuclei' [1], 'seeds' [2], or 'initiation sites' [3] and proceeds stepwise to the natively folded protein [4,5]. In contrast to the successive protein folding process, protein unfolding is a highly cooperative reaction. Consequently, intermediates are much less frequently populated here [6]. Due to the principle of microscopic reversibility, however, unfolding is a stepwise process as well, which is postulated to start at confined regions of the tertiary structure of the native protein molecule [7]. In fact, numerous studies accumulate evidence for the existence of suchlike regions, which accordingly were termed 'unfolding region' [8,9], 'critical region' [10], 'unfolding nucleation site' [11], or similar.

The rate constants of the folding (k_f) and unfolding (k_U) reaction, both of which determine the respective free energy of activation $\Delta G_f^{\ddagger}$ and $\Delta G_U^{\ddagger}$ and, thus, the Gibbs free energy ΔG, provide information on the contribution of these reactions to the thermodynamic stability [12]. The comparison of proteins with their chemically modified or genetically engineered variants yields information on the involvement of specific residues in the folding or unfolding reaction. This approach has resulted in the Φ-value ($\Delta\Delta G^{\ddagger}/\Delta\Delta G$) analysis by Fersht and coworkers to evaluate the native-like arrangement of specific residues in the transition state [13,14]. As a consequence, modifications in the folding region should influence ΔG by changing k_f ($\Delta G_f^{\ddagger}$) whereas modifications in the unfolding region should influence ΔG by changing k_U ($\Delta G_U^{\ddagger}$).

Proteins from thermophilic organisms structurally differ from their mesophilic homologues by an increase in the number of native contacts (increase in ΔG by stabilizing the native state N) or by the introduction of proline residues and disulfide bonds. According to the chain entropy model [15–17], introduced proline residues and disulfide bonds are considered to increase ΔG by an entropic destabilization of the unfolded state [18–20]. However, particularly introduced disulfide bonds may affect the native state as well since they might prevent unfolding by tethering the native protein structure [21].

Bovine pancreatic ribonuclease A (RNase A) is one of the most thoroughly studied model proteins concerning the protein folding problem. The folding region of RNase A had been postulated for residues 106–118 (Fig. 1; [22]) and its importance for the folding and stability of the RNase A molecule has been confirmed by mutagenesis studies [23] or replacement of *cis*Pro114 by the *cis*-locked β-turn mimic 5′,5′-dimethylproline [24]. As for the unfolding process, the section from the C-terminal end of helix II (Lys31) through the first β-sheet strand (Phe46) became susceptible first to proteolytic attack by thermolysin and trypsin under denaturing conditions [25] and several residues in this region showed a faster H–D exchange than that of global unfolding [26,27]. The designation of this region as unfolding region of RNase A was confirmed by both computer simulations and studies using either the glycosylated variant of RNase A, RNase B, or genetically engineered RNase A variants [28–30].

Abbreviations: AUAA, 6-carboxyfluorescein-dArU(dA)$_2$-6-carboxytetramethylrhodamine; DTNB, 5,5′-dithiobis-(2-nitrobenzoic acid); GdnHCl, guanidine hydrochloride; ONC, onconase; RNase, ribonuclease.

* Corresponding author. Tel.: +49 345 5524865; fax: +49 345 5527303.
E-mail address: ulrich.arnold@biochemtech.uni-halle.de (U. Arnold).
URL: http://www.biochemtech.uni-halle.de/biotech (U. Arnold).

0301-4622/$ – see front matter © 2008 Elsevier B.V. All rights reserved.
doi:10.1016/j.bpc.2008.12.005

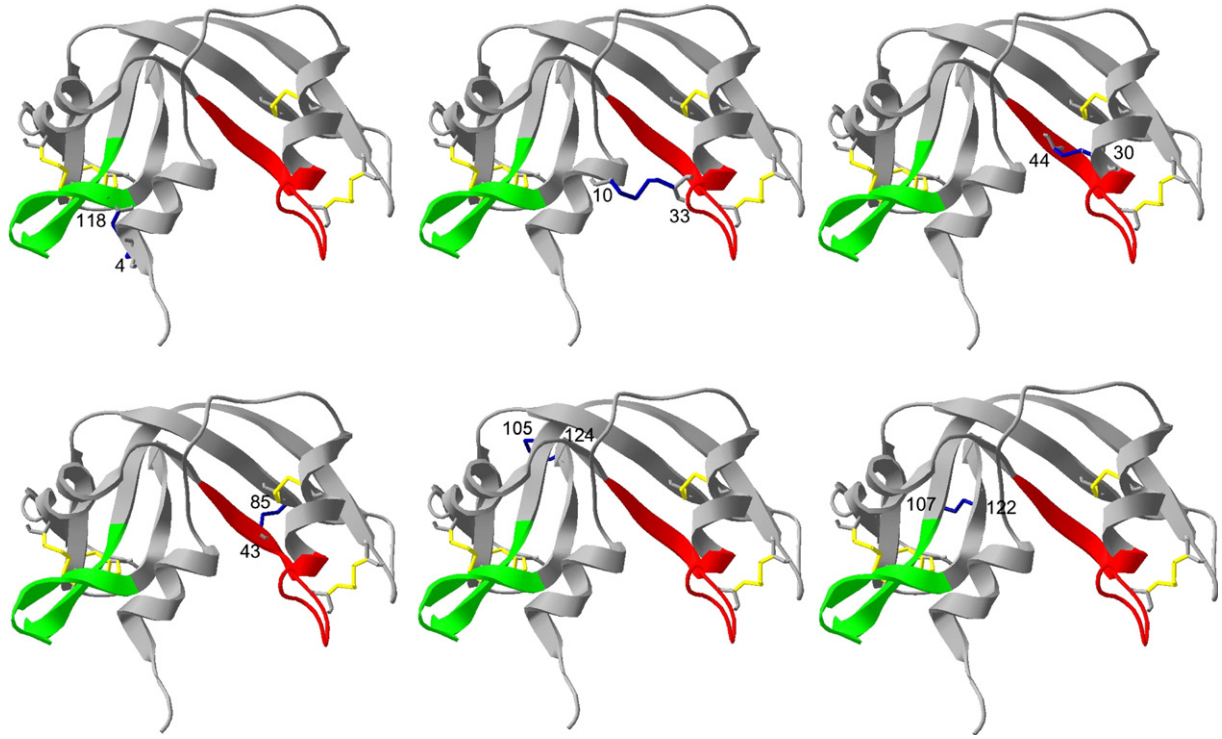

Fig. 1. Tertiary structure of RNase A with the introduced disulfide bonds. The model (7rsa) was taken from the Brookhaven protein data bank and drawn with Swiss pdb-Viewer v3.7. In addition to the native disulfide bonds (yellow), the position of the respective additional disulfide bond 4–118, 10–33, 30–44, 43–85, 105–124, or 107–122 is indicated in blue. Furthermore, the proposed folding region (residues 106–118, [22]) and unfolding region (residues 31–46, [25]) are indicated in green and red, respectively, labeling R10C/R33C-, M30C/N44C-, and V43C/R85C-RNase A as unfolding variants and A4C/V118C-, H105C/V124V-, and I107C/A122C-RNase A as folding variants (For interpretation of the references to colour in this figure legend, the reader is referred to the web version of this article).

RNase A contains four disulfide bonds that tether the protein molecule (Fig. 1) and considerably contribute to its thermodynamic stability. Replacement of single cystines diminished the transition temperature T_m by about 20–36 °C [31,32]. In reversal, an 1,5-difluoro-2,4-dinitrobenzene cross-link between Lys7 and Lys41 [33] increased T_m by 25 °C [34] or 12.5 kJ mol^{-1} [35], which was almost exclusively caused by a deceleration of the unfolding reaction ($\Delta\Delta G_U^{\ddagger} \approx 11$ kJ mol^{-1}, [35]). Introduction of an additional disulfide bond by genetic engineering into human pancreatic RNase 1 (R4C/V118C-RNase 1) increased ΔG by 9 kJ mol^{-1} [36] and the analog disulfide bond in A4C/G88R/V118C-RNase A increased T_m by 4.8 °C in comparison to G88R-RNase A [37]. The influence of the extra disulfide bond on the folding behavior of the RNase, however, has not been studied. Interestingly, in onconase (ONC), a homolog of RNase A with strongly reduced k_U in comparison to RNase A [38], three out of the four disulfide bonds of RNase A are conserved. The forth disulfide bond, which tethers the C-terminus of ONC to the protein body, significantly contributes to the stability of ONC as its replacement by a pair of alanines reduces the stability of ONC by 32 kJ mol^{-1} due to an increase in k_U and a decrease of k_f [38].

In a recent study [39], we have investigated the thermal unfolding of A4C/V118C- and V43C/R85C-RNase A as variants with additional cross-links in the folding and unfolding region of RNase A, respectively. In contrast to the expectation from the chain entropy model, the increase in stability (ΔT_m=+4.9 °C and +2.2 °C, respectively) was found to result mainly from a decrease in k_U in both variants. More recently, Pradeep et al. [40] have studied the same variants in guanidine hydrochloride (GdnHCl) and confirmed the decrease of k_U observed under thermal denaturation. While no change in k_f was found for V43C/R85C-RNase A (confirming the expectations from thermal denaturation), folding of A4C/V118C-RNase A was found to be decelerated by almost the same extent as k_U. Even though these counteracting effects should compensate for any effect on ΔG, T_m was found to be increased by about 6 °C.

Here we extend our previous studies by four additional variants modifying both the folding and unfolding region of RNase A. Equilibrium unfolding studies are correlated to folding/unfolding kinetics to dissect the effect of the introduced disulfide bonds on the unfolded, transition, and native state, respectively. In contrast to the expectation, in all variants mainly the unfolding reaction is affected. The extent of the effect, however, strongly depends on the position of the newly introduced disulfide bond.

2. Materials and methods

2.1. Materials

Oligonucleotides and 6-carboxyfluorescein-dArU(dA)$_2$-6-carboxy-tetramethylrhodamine (AUAA) were from metabion international AG, Martinsried, Germany. RNase A was from Sigma, Taufkirchen, Germany, restriction enzyme *Dpn*I was from New England Biolabs, Frankfurt/Main, Germany, growth media were from Difco Laboratories, Detroit, MI, USA, and *Escherichia coli* (*E. coli*) strains XL-1 Blue and BL21(DE3) were from Stratagene, Heidelberg, Germany. All other chemicals were of purest grade commercially available.

2.2. Site-directed mutagenesis

The *rnase A* gene in pET-26b(+) [41] was modified by use of the QuikChange™ site-directed mutagenesis kit (Stratagene) to obtain the mutations A4C/V118C, R10C/R33C, M30C/N44C, V43C/R85C, H105C/V124C, and I107C/A122C. The mutations were introduced in two steps except for M30C/N44C (one step, see Table S-1) and verified by DNA sequencing according to Sanger et al. [42] using the SequiThermExcel™ LongRead™ DNA sequencing kit (Biozym, Hess. Oldendorf, Germany) and a Li-COR 4000 DNA-sequencer (MWG Biotech, Ebersberg, Germany).

2.3. Expression, renaturation, and purification of the enzyme variants

The experimental procedures were performed as described previously [29,41]. Removal of protein species with incomplete disulfide bond formation was achieved by addition of 10-fold molar excess of 5,5′-dithiobis-(2-nitrobenzoic acid) (DTNB; 100 mM, dissolved in 50 mM Tris–HCl, pH 7.5). After 2 h of incubation at room temperature, chromatography on the SOURCE S column was repeated to remove the reacted material.

2.4. Determination of the protein concentration

The protein concentration was determined using the extinction coefficient of ε = 9800 M^{-1} cm^{-1} at 278 nm for RNase A and 9 940 M^{-1} cm^{-1} for the disulfide variants according to the calculations by Pace et al. [43].

2.5. Catalytic activity

Values of k_{cat}/K_M for the enzymatic cleavage of the fluorogenic substrate AUAA were determined as described previously [44]. Activity was measured at 20 °C in 100 mM 2-(*N*-morpholino) ethanesulfonic acid-NaOH buffer (pH 6.0) containing NaCl (100 mM).

2.6. Circular dichroism (CD) spectroscopy

CD spectra of RNase A and its variants were recorded in 50 mM sodium phosphate buffer, pH 8.0, containing NaCl (25 mM) and 1 mg mL^{-1} of protein, on a CD spectrometer J-810 (Jasco, Groß-Umstadt, Germany) at 25 °C. Cuvettes of 1 cm and 0.01 cm path length were used for CD spectroscopy in the near-UV region (250–340 nm) and in the far-UV region (185–260 nm), respectively.

2.7. Thermally induced transition

Values of T_m were determined by CD spectroscopy (CD spectrometer J-810, Jasco) at 278 nm using a heating rate of 0.5 K min^{-1}. Measurements were carried out in 50 mM sodium phosphate buffer, pH 8.0, containing NaCl (25 mM) and 1 mg mL^{-1} of protein. The signal *y* was fitted as described by Pace et al. [45] to obtain T_m

$$y = \frac{(y_N^0 + m_N \cdot T) + (y_D^0 + m_D \cdot T) \cdot \exp\left(\frac{\Delta H_m}{R \cdot T} \cdot \frac{T - T_m}{T_m}\right)}{1 + \exp\left(\frac{\Delta H_m}{R \cdot T} \cdot \frac{T - T_m}{T_m}\right)} \quad (1)$$

where y_N^0 and y_D^0 are the intercepts and m_N and m_D are the slopes in the pre- and post-transition region, respectively, in the *y vs. T* graph, *R* is the gas constant, *T* is the absolute temperature, and ΔH_m is the van't Hoff enthalpy at the transition midpoint.

2.8. Determination of the rate constant k_U of thermal unfolding

As RNase A is degraded by thermolysin under denaturing conditions only, values of k_U could be determined by proteolysis with thermolysin as described previously [46,47] at 35–60 °C. In a typical experiment, 20 µL of thermolysin (2 mg mL^{-1} in 50 mM Tris–HCl buffer, pH 8.0, containing 10 mM $CaCl_2$) were added to 160 µL of 50 mM Tris–HCl buffer (pH 8.0), which had been pre-incubated in a thermostat (Lauda, Lauda-Königshofen, Germany, accuracy ±0.1 °C). Reaction was started by addition of the respective RNase A variant (20 µL of a 1.0 mg mL^{-1} solution). After distinct time intervals, 20 µL were taken and mixed rapidly with 7 µL of 50 mM EDTA. Densitometric evaluation of the bands after SDS–PAGE was carried out as described previously [47]. From the decrease in the peak area of the intact RNase A band, which followed a first-order reaction, the rate constant of proteolysis k_p was determined. Under the conditions applied, these values correspond to the respective unfolding rate constants. By use of the Eyring equation, the activation enthalpy $\Delta H^{\ddagger}$ and the activation entropy $\Delta S^{\ddagger}$ were determined.

2.9. Proteolytic fragmentation under native and unfolding conditions

RNase A is cleaved by proteinase K under native conditions at the Ala20-Ser21 peptide bond. To evaluate the structural integrity of the disulfide variants in comparison to RNase A, to 160 µL Tris–HCl buffer (50 mM, pH 8.0), 20 µL of proteinase K (0.1 mg mL^{-1} in 50 mM Tris–HCl buffer, pH 8.0, containing 10 mM $CaCl_2$) and 20 µL of RNase A or its variants (1.0 mg mL^{-1}) were added. After distinct time intervals of incubation at room temperature, 18 µL were taken and mixed rapidly with 6 µL of 50 mM phenylmethylsulfonyl fluoride (dissolved in 2-propanol). Values of k_p were determined as described above. Primary cleavage of RNase A by proteinase K yields the fragments Lys1-Ala20 and Ser21-Val124 [48]. The rate constant of the formation of the fragments corresponds to k_p of the intact protein. The formation and subsequent degradation of the fragment Ser21-Val124 can be followed and described by a consecutive reaction [49]

$$A_t = A_0 \times k_p \times \left(\exp(-k_p \times t) - exp(-k_{p'} \times t)\right) / (k_{p'} - k_p) \quad (2)$$

where A_t is the band intensity at time *t*, A_0 is the fitted value for $t = 0$ s, and $k_{p'}$ is the rate constant of the degradation of the fragment.

Moreover, fragmentation of RNase A or its variants under unfolding conditions was performed with thermolysin. To 160 µL Tris–HCl buffer (50 mM, pH 8.0, incubated at that temperature where the proteins unfold with a rate constant of about 0.25 s^{-1}), 20 µL of thermolysin (0.005 mg mL^{-1} in 50 mM Tris–HCl buffer, pH 8.0, containing 10 mM $CaCl_2$) and 20 µL of RNase A or its variants (1.0 mg mL^{-1}) were added. After distinct time intervals, 25 µL were taken and mixed rapidly with 8 µL of 50 mM EDTA. After SDS–PAGE, the fragment bands were visualized by silver staining.

2.10. GdnHCl-induced transition curves and determination of the parameters of the thermodynamic stability

GdnHCl-induced transition curves of RNase A and its variants were obtained by CD spectroscopy (CD spectrometer J-810, Jasco) at 278 nm (signal was averaged over 30 s). Measurements were carried out at 25 °C in 50 mM sodium phosphate buffer, pH 8.0, containing NaCl (25 mM), 1 mg mL^{-1} of protein and 0.0–6.0 M GdnHCl. To calculate values of $[D]_{50\%}$, the concentration of denaturant at which 50% of the protein is unfolded, the signals y were fitted by nonlinear regression according to Santoro and Bolen [50] as described previously [38,51].

2.11. Folding experiments in GdnHCl

All experiments were performed at 25 °C in 50 mM sodium phosphate buffer, pH 8.0, containing NaCl (25 mM), on a Fluoro-Max-3 spectrometer (Horiba Jobin Yvon, Munich, Germany). Protein samples were preincubated in 0 or 6 M GdnHCl at 25 °C. Unfolding and refolding was initiated by manual addition of these solutions into buffer containing GdnHCl to yield the respective final GdnHCl concentration. The final protein concentration was 50 µg mL^{-1}. The band width was 5 nm for excitation at 278 nm and 5 nm for emission at 303 nm. The observed rate constants k_{obs}, which are the sum of the respective k_U and k_f values, were calculated from the change of the intensity of the emission signal as a function of time which followed first-order kinetics. The data in the resulting chevron plot ($\ln k_{obs}$ *vs.* $[D]$) were fitted according to Maxwell et al. [52]

$$\ln k_{obs} = \ln\left(\exp\left(\ln k_f^0 + m_f \cdot [D]/RT\right) + \exp\left(\ln k_U^0 + m_U \cdot [D]/RT\right)\right) \quad (3)$$

Table 1
Calculated structural parameters and catalytic activity of RNase A and its disulfide variants

RNase A variant	Distance of C_α-atoms of native residues (Å)[a]	Distance of C_β-atoms of native residues (Å)[b]	Number n of residues within the formed loop	Calculated $\Delta\Delta G^{(25\ °C)}$ (kJ mol^{-1})	Relative activity (%)
RNase A	–	–	–	–	100[c] ± 12
A4C/V118C	5.34	3.97	115	20.3	18 ± 5
R10C/R33C	6.17	5.49	24	14.4	23 ± 8
M30C/N44C	8.19	6.43	15	12.7	0.07 ± 0.03
V43C/R85C	4.73	5.74	43	16.6	20 ± 7
H105C/V124C	5.28	5.14	20	13.8	9 ± 2
I107C/A122C	5.15	4.46	16	12.9	6 ± 3

Distances were determined from the crystal structure (PDB entry 7rsa). The effect of the extra disulfide bond on ΔG at 25 °C in comparison to RNase A was calculated according to Pace et al. with constant ΔH and $\Delta S = (-8.79 - 1.5 \times R \times \ln n)$ with R being the gas constant in kJ mol^{-1} K^{-1} and n the number of residues within the formed loop [63]. Activity was determined with AUAA as substrate at 20 °C as described in Materials and methods.

[a] Distances between C_α-atoms in disulfide bonds can vary from 4.6 Å to 7.4 Å [16].

[b] Distances between C_β-atoms in disulfide bonds can vary from 2.9 Å to 4.6 Å [53].

[c] 100% correspond to a k_{cat}/K_M value of 1.74×10^7 M^{-1} s^{-1}.

where k_f^0 and k_U^0 are the rate constants of the folding and unfolding reaction in the absence of denaturant, m_f and m_U are the slopes of the folding and unfolding limbs, and R is the gas constant.

3. Results

3.1. Design of the RNase A disulfide variants

RNase A disulfide variants were designed to probe the influence of additional disulfide bonds on the stability and folding behavior of RNase A. The positions of the additional disulfide bonds, which were to be introduced into the folding or unfolding region of RNase A (Fig. 1), were determined from the crystal structure of RNase A (PDB entry 7rsa) by use of the program SSBOND [53] or by determination of the distances of the C_α- and C_β-atoms (Table 1) of the respective residues. Additional positions that might result from the analysis of solution structures [54] as well as conformational perturbations by the cysteine substitutions were not considered. As a result, six variants out of in total 27 possible candidates were considered as promising with each three concerning the folding (A4C/V118C, H105C/V124C, and I107C/A122C) or unfolding region (R10C/R33C, M30C/N44C, and V43C/R85C), respectively (Fig. 1). Even though the distances between the C_α- and C_β-atoms of Met30 and Asn44 (8.2 Å and 6.4 Å) were larger than for disulfide bonds and, thus, the formation of a disulfide bond was expected to result in a deformation of the protein backbone, this variant was selected as it directly cross-links the unfolding region of the RNase A molecule. As the disulfide bonds 105–124 and 107–122 tether the C-terminus to the protein body they mimic the C-terminal disulfide bond in ONC. The importance of this disulfide bond for the stability and folding of this RNase A homolog had been demonstrated previously [38]. According to the chain entropy model, the loss of entropy in the unfolded state should result in a thermodynamic stabilization of all variants (Table 1).

3.2. Expression, renaturation, and purification

All RNase A disulfide variants were expressed as inclusion bodies, renatured, and purified as described in Materials and methods. Even though differing in their tendency to form aggregates during renaturation, all variants could be obtained in sufficient amounts (up to 10 mg L^{-1} of culture medium). After the first chromatography on a SOURCE S column and addition of DTNB, mass spectrometry showed that the amount of molecules w only partial formation of disulfide bonds differed considerably among the variants depending on the position of the mutation. The DTNB-modified species were eluted at lower NaCl concentrations in the second chromatography and, thus, could be eliminated. The finally collected material did not react with DTNB indicating the formation of all disulfide bonds. Furthermore, as scrambled RNase A, *i.e.* RNase A with incorrect disulfide bonds, lacks catalytic activity [55] and all variants proved to be catalytically active, we suppose a correct disulfide bond formation. Mass spectrometry also indicated a complete formation of all disulfide bonds (Table S-2) and the purified proteins proved to be homogeneous by SDS–PAGE and re-chromatography.

3.3. Activity

The k_{cat}/K_M values for RNase A and its variants, determined with AUAA as substrate, revealed that all RNase A disulfide variants were less active than RNase A with M30C/N44C-RNase A being least active (Table 1). Interestingly, fractions of M30C/N44C-RNase A that vividly reacted with DTNB indicating the lack of at least one disulfide bond (most likely 30–44 according to the distance between the C_α- and C_β-atoms of Met30 and Asn44, Table 1) were fully active (data not shown). As all extra disulfide bonds are located more or less in the vicinity of active site residues (His12, Lys41, and His119), this decrease of activity is not surprising.

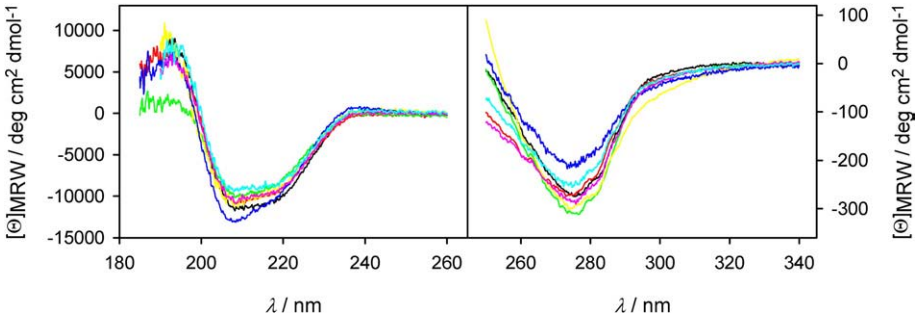

Fig. 2. CD spectra of RNase A and its disulfide variants. Far-UV (left) and near-UV (right) CD spectra of RNase A (—) and its variants A4C/V118C (—), R10C/R33C (—), M30C/N44C (—), V43C/R85C (—), H105C/V124V (—), and I107C/A122C (—) were recorded in 50 mM sodium phosphate buffer, 25 mM NaCl, pH 8.0, at 25 °C using a protein concentration of 1 mg mL^{-1} as described in Materials and methods.

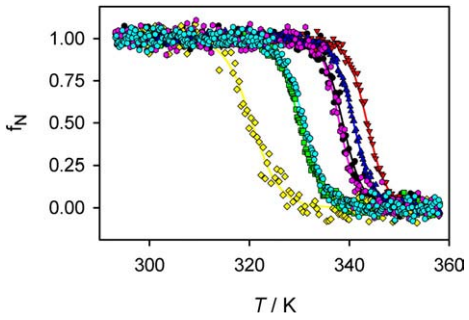

Fig. 3. Thermally induced transition of RNase A and its disulfide variants. Transition curves (fraction of native protein f_N as a function of temperature) of RNase A (●) and its variants A4C/V118C (▼), R10C/R33C (■), M30C/N44C (◆), V43C/R85C (▲), H105C/V124 V (⬟), and I107C/A122C (⬟) were recorded by CD spectroscopy at 278 nm in 50 mM sodium phosphate buffer, 25 mM NaCl, pH 8.0, using a protein concentration of 1 mg mL^{-1} as described in Materials and methods.

3.4. CD spectra

As deduced from the concordant CD spectra in the far- and near-UV region, all RNase A variants acquire a secondary and tertiary structure comparable to that of RNase A (Fig. 2). The most pronounced deviation is observed for M30C/N44C-RNase A, the variant with the least catalytic activity.

3.5. Thermally induced transition

The thermal stability of RNase A and its variants was investigated by CD measurements (Fig. 3). Thermal unfolding proved to be reversible and follows a two-state transition model as judged from the fit of the data. While H105C/V124C-RNase A, the variant with the disulfide bond homolog to ONC is as stable as RNase A and A4C/V118C- and V43C/R85C-RNase A are more stable than RNase A, R10C/R33C-, I107C/A122C-, and particularly M30C/N44C-RNase A are destabilized in comparison to RNase A (Fig. 3, Table 2). Likewise, the values of ΔH_m were significantly diminished for the latter three variants (Table 3).

3.6. Thermally induced unfolding kinetics

The increased and decreased thermodynamic stability of the RNase A variants could arise from a slower unfolding or faster refolding (or both) and *vice versa*. The kinetics of thermally induced unfolding was assessed by limited proteolysis with thermolysin under conditions where the observable rate constant of proteolysis corresponds to k_U [47]. As disulfide bonds should predominantly affect the unfolded state [15,18,56], marginal changes in k_U were expected for the disulfide variants in comparison to RNase A. In contrast, according to the unfolding region postulate k_U should account for the changes in thermal stability for the unfolding region variants (R10C/R33C-, M30C/N44C-, and V43C/R85C-RNase A). Fig. 4 shows the obtained Eyring plot which reveals a slower unfolding for both A4C/V118C- and V43C/R85C-RNase A despite the localization of these disulfide bonds in the folding and unfolding region, respectively. The comparison of the values of $\Delta\Delta G^{(T_m)}$ and $\Delta G_U^{\ddagger(T_m)}$ (Table 2) discloses that the extra disulfide bond exerts its effects completely by influencing the unfolding reaction of V43C/R85C- and H105C/V124C-RNase A, whereas $\Delta\Delta G_U^{\ddagger(T_m)}$ accounts for about 60–80% of the $\Delta\Delta G^{(T_m)}$ effect for the other variants regardless of the position of the extra disulfide bond. From the Eyring plot, $\Delta H^{\ddagger}$ and $\Delta S^{\ddagger}$ were calculated (Table 3). Like for ΔH_m, $\Delta H^{\ddagger}$ is hardly changed for A4C/V118C-, V43C/R85C-, and H105C/V124C-RNase A but it is significantly reduced for the other RNase A variants, most pronounced for M30C/N44C-RNase A. Obviously, the introduction of the extra disulfide bond results in a disturbance of the stabilizing interactions in the native protein, presumably by a deformation of the tertiary structure.

3.7. Native-state proteolysis

To assess the native conformation of the RNase A variants, proteolysis with proteinase K was carried out at room temperature. Like subtilisin [57], proteinase K degrades RNase A by primary cleavage of the Ala20-Ser21 peptide bond [48] resulting in the so-called *S*-peptide Lys1-Ala20 and the *S*-protein Ser21-Val124. These two fragments remain joined by multiple noncovalent interactions [58] and yield catalytically fully active protein, termed RNase S [57]. While A4C/V118C-, V43C/R85C-, H105C/V124C-, and I107C/A122C-RNase A were degraded with the same value of k_p as RNase A, k_p increased 2.9-fold and 4.3-fold for M30C/N44C- and R10C/R33C-RNase A, respectively (Table S-3, Fig. S-1). The obvious disturbance of the native state of these two variants, resulting in an increased proteolytic susceptibility, is consistent with the decrease in $\Delta H^{\ddagger}$ (Table 3). The time course of the primary fragment Ser21-Val124 revealed even more pronounced differences. While $k_{p'}$, *i.e.* the consecutive degradation of the S-protein (and, thus, most likely of RNase S), of V43C/R85C- and H105C/V124C-RNase A remained unaffected by the extra disulfide bond, it is decreased about 5-fold in the two variants in which S-peptide and S-protein are covalently linked (A4C/V118C- and R10C/R33C-RNase A). In contrast, $k_{p'}$ is increased 10- to 15-fold in I107C/A122C- and M30C/N44C-RNase A. In I107C/A122C-RNase A the interactions between the C-terminal β-strand and the *S*-peptide might be disturbed by the extra disulfide bond resulting in a more facile dissociation of the two fragments followed by unfolding and degradation. The consecutive degradation of the *S*-protein of M30C/N44C-RNase A showed a clear deviation

Table 2
Parameters of thermally or GdnHCl-induced unfolding of RNase A and its variants

RNase A variant	T_m (°C)	$\Delta\Delta G^{(T_m)}$ (kJ mol^{-1})[a]	$\Delta\Delta G_U^{\ddagger(T_m)}$ (kJ mol^{-1})[b]	$[D]_{50\%}$(M)	$\Delta\Delta G^{[D]_{50\%}}$(kJ mol^{-1})[c]	$\Delta\Delta G_U^{\ddagger[D]_{50\%}}$(kJ mol^{-1})[d]	$\Delta\Delta G_f^{\ddagger[D]_{50\%}}$(kJ mol^{-1})[d]
RNase A	65.6±0.1	0.0	0.0	3.1±0.1	0.0	0.0	0.0
A4C/V118C	70.5±0.1	7.3	5.8	3.6±0.2	7.1	4.7	−1.4
R10C/R33C	56.9±0.1	−11.2	−7.4	2.4±0.2	−9.9	−5.8	0.7
M30C/N44C	47.4±0.2	−21.1	−12.2	n.d.	n.d.	n.d.	n.d.
V43C/R85C	67.8±0.1	3.2	4.2	3.6±0.1	7.1	4.2	−1.4
H105C/V124C	64.9±0.1	−1.0	−1.9	3.1±0.1	0.0	−0.5	0.4
I107C/A122C	57.8±0.1	−10.2	−7.1	2.3±0.1	−11.4	−9.5	1.5

Values of T_m and $[D]_{50\%}$ were determined as described in Materials and methods. $\Delta\Delta G^{(T_m)}$ and $\Delta\Delta G^{[D]_{50\%}}$ are the differences in free energy between an RNase A variant and RNase A at T_m and $[D]_{50\%}$ of the respective variant. $\Delta\Delta G_U^{\ddagger(T_m)}$ and $\Delta\Delta G_U^{\ddagger[D]_{50\%}}$ are the differences in free energy of activation of the unfolding reaction between an RNase A variant and RNase A at T_m and $[D]_{50\%}$ of the respective variant, $\Delta\Delta G_f^{\ddagger[D]_{50\%}}$ is the difference in free energy of activation of the folding reaction between an RNase A variant and RNase A at $[D]_{50\%}$ of the respective variant.

[a]Calculated by means of the modified Gibbs–Helmholtz equation [45] with (479±20) kJ mol^{-1} for ΔH_m (Table 3) and (9.4±0.06) kJ mol^{-1} K^{-1} for ΔC_p [47]; the resulting error is <10%.
[b]Calculated from values of k_U by means of the Eyring equation; the resulting error is <15%.
[c]Calculated by the linear extrapolation method [45]; the resulting error is <10%.
[d]Calculated from values of k_U or k_f, respectively, which were obtained by use of Eq. (3) from the chevron plot [52], by means of the Eyring equation; the resulting error is <15%.

Table 3
Thermodynamic and kinetic parameters of thermally or GdnHCl-induced unfolding of RNase A and its variants

RNase A variant	ΔH_m (kJ mol^{-1})	ΔS_m (J mol^{-1} K^{-1})	$\Delta H^{\ddagger}$ (kJ mol^{-1})	$\Delta S^{\ddagger}$ (J mol^{-1} K^{-1})	$m_{\Delta G}$ (kJ mol^{-1} M^{-1})	$\lvert m_f \rvert$ (kJ mol^{-1} M^{-1})	m_U (kJ mol^{-1} M^{-1})
RNase A	479±20	1415±59	342±11	754±34	13.92±0.84	2.65±0.08	8.33±0.64
A4C/V118C	492± 9	1431±27	304±18	625±55	11.87± 1.14	2.09±0.09	5.37±0.39
R10C/R33C	410± 7	1242±21	224± 6	419±20	10.05±0.63	1.98±0.16	8.40±0.82
M30C/N44C	312±16	974±51	179±21	284±65	n.d.	n.d.	n.d.
V43C/R85C	487± 8	1429±23	312±19	653±57	10.69±1.29	2.13±0.10	8.36±0.55
H105C/V124C	538±24	1592±72	326± 2	712± 7	12.91±0.80	2.84±0.19	6.91±0.73
I107C/A122C	413± 9	1246±28	250±19	497±59	9.96± 0.83	3.28±0.20	6.02±0.34

ΔH_m was determined from the thermally induced transition curves (Fig. 3) by use of Eq. (1) and ΔS_m, the entropy at T_m, was calculated according to $\Delta S_m = \Delta H_m/T_m$. $\Delta H^{\ddagger}$ and $\Delta S^{\ddagger}$, the enthalpy and entropy of activation, were determined by use of the Eyring equation from Fig. 4. Values of $m_{\Delta G}$ were determined from GdnHCl-induced transition curves (Fig. 5) according to [45] and values of m_f and m_U were determined from the chevron plot (Fig. 6) with Eq. (3) according to [52].

from a first-order reaction. Steric shielding of the next cleavage sites resulting in a second-order reaction or aggregation of the M30C/N44C-RNase S might be a reason of this deviation.

3.8. Fragmentation under unfolding conditions

Incubation of RNase A in the presence of trypsin or thermolysin at 60–65 °C results in a fast degradation of RNase A and an accumulation of primary fragments [25]. The identified primary cleavage sites (Asn34-Leu35 and Thr45-Phe46 for thermolysin) thereby mark the unfolding region, *i.e.* that region where the unfolding process is initiated. To assess the initiation of unfolding of the RNase A disulfide variants in comparison to RNase A, the proteins were incubated in the presence of thermolysin at that temperature where $k_U \approx 0.25\ s^{-1}$ (*e.g.* 65 °C for RNase A). All variants showed the same fragmentation pattern but the intensity of the fragments 35–124 (R10C/R33C-RNase A) and 46–124 (M30C/N44C- and V43C/R85C-RNase A) was considerably decreased due to a shielding of the respective cleavage sites by the extra disulfide bonds (Fig. S-2). Nevertheless, the results indicate no significant change in the initiation of the unfolding pathway of the RNase A variants in comparison to RNase A.

3.9. GdnHCl-induced transition

To study the effect of the extra disulfide bonds on the thermodynamic stability of the RNase A molecule, GdnHCl-induced transition curves were recorded (Fig. 5). By reason of the absence of a linear pre-transition signal for the variant M30C/N44C-RNase A in GdnHCl, we abstained from further studies concerning this variant. Again, the introduction of the additional disulfide bonds resulted in a more or less pronounced loss of steepness in the transition curve ($m_{\Delta G}$, Table 3). The values of $[D]_{50\%}$ and the change in standard free energy at the transition midpoint ($\Delta\Delta G^{[D]_{50\%}}$) are summarized in Table 2. The order of the degree of stabilization/destabilization as the result of the amino acid substitutions was the same as for the thermally induced unfolding.

3.10. Folding experiments in GdnHCl

As under thermally induced unfolding, changes in k_U and/or k_f should be responsible for changes in the thermodynamic stability of the RNase A variants in comparison to RNase A. To dissect the effect of the extra disulfide bonds, rate constants of unfolding and refolding of RNase A and its variants were determined by fluorescence spectroscopy with GdnHCl as denaturant (Fig. 6). Only the conformational unfolding phase and the main refolding phase (the folding of the major slow-refolding species U_S^{II}) were considered here as the folding of U_S^{II} dominates the folding of RNase A within the transition region [59,60]. Because of the occurrence of a native-like intermediate due to a rate-limiting proline *cis*/*trans* isomerization step, measurements were carried out at 25 °C where isomerization is faster than folding and, thus, does not interfere with the folding reaction [61]. For RNase A, the values determined here are consistent with those reported earlier [61]. The early hydrogen-bonded intermediate I_1 in the folding of U_S^{II} is not detected by fluorescence spectroscopy [61].

Surprisingly but confirming the results from thermal unfolding, despite of the different positions of the introduced disulfide bonds the main effect was observed for the unfolding reaction whereas the folding reaction was much less affected for both the folding region and unfolding region variants. From k_f and k_U at the respective transition midpoint (Figs. 5 and 6), values of $\Delta\Delta G_U^{\ddagger[D]_{50\%}}$ and $\Delta\Delta G_f^{\ddagger[D]_{50\%}}$ were calculated for each variant (Table 2). The values clearly indicate that the effect on the thermodynamic stability of the variants has mainly to be attributed to an effect on the unfolding reaction. The values of $\Delta\Delta G$ calculated from the kinetic data ($\Delta\Delta G = \Delta\Delta G_U^{\ddagger[D]_{50\%}} - \Delta\Delta G_f^{\ddagger[D]_{50\%}}$) slightly deviate from $\Delta\Delta G$ calculated from the thermodynamic data (as do the values of $m_{\Delta G}$ and $|m_f|+m_U$, Table 3) due to presence of further minor kinetic phases in the folding of RNase A. Interestingly, all three

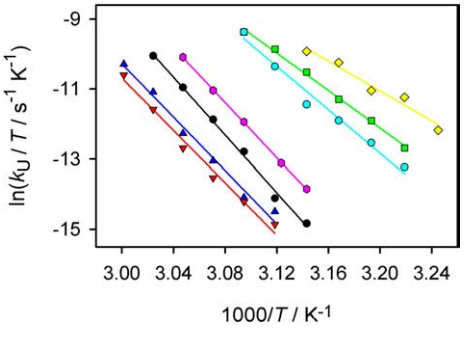

Fig. 4. Eyring plot of RNase A and its disulfide variants. Unfolding rate constants of RNase A (●) and its variants A4C/V118C (▼), R10C/R33C (■), M30C/N44C (), V43C/R85C (▲), H105C/V124V (⬟), and I107C/A122C (⬟) were determined by limited proteolysis with thermolysin in 50 mM Tris–HCl buffer, pH8.0, using a final protein concentration of 100 μg mL^{-1} as described in Materials and methods.

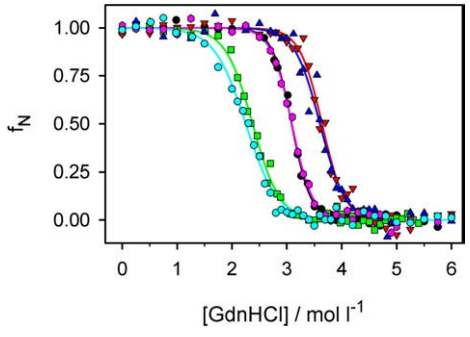

Fig. 5. GdnHCl-induced transition of RNase A and its disulfide variants. Transition curves (fraction of native protein f_N as a function of the concentration of GdnHCl) of RNase A (●) and its variants A4C/V118C (▼), R10C/R33C (■), V43C/R85C (▲), H105C/V124V (⬟), and I107C/A122C (⬟) were recorded by CD spectroscopy at 278 nm in 50 mM sodium phosphate buffer, 25 mM NaCl, pH 8.0, at 25 °C using a protein concentration of 1 mg mL^{-1} as described in Materials and methods.

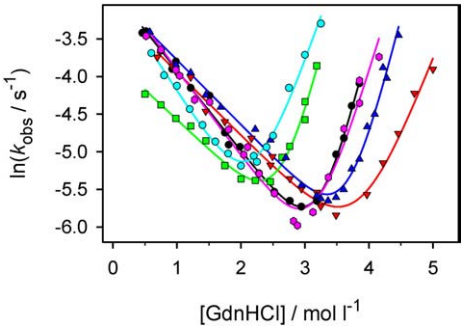

Fig. 6. Chevron plots for the unfolding and refolding of RNase A and its disulfide variants. Values of k_{obs} of RNase A (●) and its variants A4C/V118C (▼), R10C/R33C (■), V43C/R85C (▲), H105C/V124V (⬟), and I107C/A122C (⬤) were determined by fluorescence spectroscopy in 50 mM sodium phosphate buffer, 25 mM NaCl, pH 8.0, at 25 °C using a final protein concentration of 50 μg mL^{-1} as described in Materials and methods.

RNase A variants with the extra disulfide bond in the folding region show a shallower unfolding limb (m_U decreases by 17–35%) in the chevron plot (Fig. 6, Table 3) in comparison to RNase A indicating a shift of the transition state towards the native state.

4. Discussion

Disulfide bonds were shown to play a crucial role for the stability of the respective proteins as their removal by reduction or mutation results in a stability loss [16,31,62,63]. According to the chain entropy model, disulfide bonds (as well as cross-links) should increase ΔG due to an entropy loss of the unfolded polypeptide chain [15–17,63]. Thus, escape of molecules from U should be facilitated, which results in an increase in k_f, whereas k_U should basically remain unaffected. While the stability loss due to the elimination of native disulfide bonds in proteins mostly meets the expectations, the introduction of additional disulfide bonds into proteins yielded contradictory results. Various proteins in fact could be stabilized by an extra disulfide bond [56,64–68] whereas others showed no effect or were even destabilized [64,69–71] with a strong dependence on the position of the introduced disulfide bond [65,67]. Thus, a calculation of $\Delta\Delta G$ based on $\Delta\Delta S$ (from the tethering of the loop) only is not sufficient but hydrophobic effects of disulfide bonds and enthalpic effects on the folded protein have to be considered as well [17,21]. Moreover, the introduction of disulfide bonds might cause 'disulfide-induced strain in the folded state' [21,56,70] and preexisting disulfide bonds impair the calculability of $\Delta\Delta S$ and $\Delta\Delta G$ [15,56]. Furthermore, extra disulfide bonds may change the folding and unfolding pathways [67] or even result in kinetic traps due to non-productive interactions [72]. Interestingly and in contrast to the expectation from the chain entropy model, the main effect on ΔG usually was found to be exerted by affecting the unfolding reaction [66–68].

Starting from the proposed folding region (residues 106–118, [22]) and unfolding region (residues 31–46, [25]) of RNase A, we introduced extra disulfide bonds and studied the effect on the thermodynamic stability and folding/unfolding reaction of the variants in comparison to RNase A. Regardless of the position of the extra disulfide bond, the main effect for both stabilized and destabilized variants was exerted *via* k_U (Figs. 4 and 6, Table 2). It is noteworthy that at least the initiation of the unfolding process, however, remains unchanged as deduced from the proteolytic fragmentation patterns by thermolysin.

In contrast to the propositions for the Φ-value analysis [13,14], changes of the unfolded state by extra disulfide bonds have to be considered here as well. Two of the three variants with the extra disulfide bond in the unfolding region, R10C/R33C- and M30C/N44C-RNase A (Fig. 1), were destabilized in comparison to RNase A under thermally induced denaturation by affecting both k_U and k_f (Fig. 4, Table 2). Here, the disturbance of the native state, indicated by the increased susceptibility to proteinase K and the decreased values for $\Delta H^{\ddagger}$, as well as an perturbation of the folding reaction obviously countervail the theoretic entropy gain in the unfolded state. Despite the expected preformation of the folding region 106–118 in the folding variants I107C/A122C-RNase A and H105C/V124-RNase A (Fig. 1), the variants analog to ONC, which is more stable than RNase A by 20 kJ mol^{-1}, no increase in k_f was observed. Rather, while ΔG of H105C/V124-RNase A remained unaffected, I107C/A122C-RNase A was considerably destabilized due to an increase in k_U (Figs. 4 and 6, Table 2), which is caused by a disturbance of the native state as indicated by the increased susceptibility of I107C/A122C-RNase S to proteinase K ($k_{p'}$, Table S-3) as well as by the decrease of $\Delta H^{\ddagger}$ (Table 3). A4C/V118C-RNase A, the variant with the longest loop between the two cysteines, is the most stable variant even though the increase by (7.2 ± 0.1) kJ mol^{-1} (Table 2) is smaller than the calculated value of 20.3 kJ mol^{-1} (Table 1). Even though designed as a folding variant (Fig. 1), more than two thirds of the increase in ΔG are caused by a decrease in k_U (*i.e.* an increase in $\Delta G_U^{\ddagger}$). As native-state proteolysis (Fig. S-1, Table S-3) is not affected by the extra disulfide bond, the stabilization of this variant is attributed to a congeneric destabilization of both the unfolded and the transition state. Finally, in V43C/R85C-RNase A the unfolding region is tethered to the protein body (Fig. 1). Here (at least for thermally induced unfolding), the increase in ΔG is completely caused by an increase in $\Delta G_U^{\ddagger}$ (Table 2) providing experimental support for both the model of the unfolding region [8,9] and the proposed unfolding region in RNase A [25,28,29].

In summary, in contrast to the effect of the elimination of native disulfide bonds, the effect of the introduction of additional disulfide bonds is much harder to predict due to an impact on both the unfolded and the native state of the protein. Accordingly, extra disulfide bonds can exert their effect not only by a destabilization of U but *via* k_U or k_f (or both). The stabilizing or destabilizing effect of the extra disulfide bond obviously depends more on the position rather than on the loop size between the cysteine residues [21,65]. When the subtle network of interactions of the native state is not impaired, the introduction of disulfide bonds is a potent tool for increasing a protein's stability.

Acknowledgments

The authors thank Dr. Sabine Gebauer (Martin-Luther University Halle-Wittenberg, Germany, current address: Bayer Bitterfeld GmbH, Germany) for modeling of disulfide variants of RNase A as well as Dr. Bart Hazes (University of Alberta, Edmonton, Alberta, Canada) for running the program SSBOND. Dr. A. Schierhorn (Martin-Luther University Halle-Wittenberg, Germany) is acknowledged for performing mass spectrometry measurements.

Appendix A. Supplementary data

Supplementary data associated with this article can be found, in the online version, at doi:10.1016/j.bpc.2008.12.005.

References

[1] D.B. Wetlaufer, Nucleation, rapid folding, and globular intrachain regions in proteins, Proc. Natl. Acad. Sci. U. S. A. 70 (1973) 697–701.
[2] R.L. Baldwin, Seeding protein folding, Trends Biochem. Sci. 11 (1986) 6–9.
[3] A.R. Fersht, A. Matouschek, J. Sancho, L. Serrano, S. Vuilleumier, Pathway of protein folding, Faraday Discuss. (1992) 183–193.
[4] H. Roder, W. Colón, Kinetic role of early intermediates in protein folding, Curr. Opin. Struct. Biol. 7 (1997) 15–28.
[5] R.L. Baldwin, Protein folding from 1961 to 1982, Nat. Struct. Biol. 6 (1999) 814–817.
[6] T. Kiefhaber, R.L. Baldwin, Kinetics of hydrogen bond breakage in the process of unfolding of ribonuclease A measured by pulsed hydrogen exchange, Proc. Natl. Acad. Sci. U. S. A. 92 (1995) 2657–2661.
[7] V. Daggett, Molecular dynamics simulations of the protein unfolding/folding reaction, Acc. Chem. Res. 35 (2002) 422–429.
[8] R. Ulbrich-Hofmann, R. Golbik, W. Damerau, in: W.J.J. van den Tweel, A. Harder, R.M. Buitelaar (Eds.), Stability and stabilization of enzymes, Fixation of the unfolding region—a hypothesis of enzyme stabilization, Elsevier, Amsterdam, 1993, p. 497.

[9] R. Ulbrich-Hofmann, U. Arnold, J. Mansfeld, The concept of the unfolding region for approaching the mechanisms of enzyme stabilization, J. Mol. Catal. B 7 (1999) 125–131.
[10] V.G. Eijsink, O.R. Veltman, W. Aukema, G. Vriend, G. Venema, Structural determinants of the stability of thermolysin-like proteinases, Nat. Struct. Biol. 2 (1995) 374–379.
[11] S. Gåseidnes, B. Synstad, X. Jia, H. Kjellesvik, G. Vriend, V.G. Eijsink, Stabilization of a chitinase from *Serratia marcescens* by Gly->Ala and Xxx->Pro mutations, Protein Eng. 16 (2003) 841–846.
[12] S.E. Jackson, A.R. Fersht, Folding of chymotrypsin inhibitor 2. 1. Evidence for a two-state transition, Biochemistry 30 (1991) 10428–10435.
[13] A.R. Fersht, A. Matouschek, L. Serrano, The folding of an enzyme. I. Theory of protein engineering analysis of stability and pathway of protein folding, J. Mol. Biol. 224 (1992) 771–782.
[14] A.R. Fersht, S. Sato, Phi-value analysis and the nature of protein-folding transition states, Proc. Natl. Acad. Sci. U. S. A. 101 (2004) 7976–7981.
[15] D.C. Poland, H.A. Scheraga, Statistical mechanics of noncovalent bonds in polyamino acids. VIII. Covalent loops in proteins, Biopolymers 3 (1965) 379–399.
[16] J.M. Thornton, Disulphide bridges in globular proteins, J. Mol. Biol. 151 (1981) 261–287.
[17] A.J. Doig, D.H. Williams, Is the hydrophobic effect stabilizing or destabilizing in proteins? The contribution of disulphide bonds to protein stability, J. Mol. Biol. 217 (1991) 389–398.
[18] C. Vieille, G.J. Zeikus, Hyperthermophilic enzymes: sources, uses, and molecular mechanisms for thermostability, Microbiol. Mol. Biol. Rev. 65 (2001) 1–43.
[19] V.G. Eijsink, A. Bjørk, S. Gåseidnes, R. Sirevåg, B. Synstad, B. van den Burg, G. Vriend, Rational engineering of enzyme stability, J. Biotechnol. 113 (2004) 105–120.
[20] M. Sadeghi, H. Naderi-Manesh, M. Zarrabi, B. Ranjbar, Effective factors in thermostability of thermophilic proteins, Biophys. Chem. 119 (2006) 256–270.
[21] B. Tidor, M. Karplus, The contribution of cross-links to protein stability: a normal mode analysis of the configurational entropy of the native state, Proteins 15 (1993) 71–79.
[22] R.R.J. Matheson, H.A. Scheraga, A method for predicting nucleation sites for protein folding based on hydrophobic contacts, Macromolecules 11 (1978) 819–829.
[23] M.G. Coll, Protasevich, J. Torrent, M. Ribó, V.M. Lobachov, A.A. Makarov, M. Vilanova, Valine 108, a chain-folding initiation site-belonging residue, crucial for the ribonuclease A stability, Biochem. Biophys. Res. Commun. 265 (1999) 356–360.
[24] U. Arnold, M.P. Hinderaker, J. Köditz, R. Golbik, R. Ulbrich-Hofmann, R.T. Raines, Protein prosthesis: a nonnatural residue accelerates folding and increases stability, J. Am. Chem. Soc. 125 (2003) 7500–7501.
[25] U. Arnold, K.P. Rücknagel, A. Schierhorn, R. Ulbrich-Hofmann, Thermal unfolding and proteolytic susceptibility of ribonuclease A, Eur. J. Biochem. 237 (1996) 862–869.
[26] T. Kiefhaber, R.L. Baldwin, Hydrogen exchange and the unfolding pathway of ribonuclease A, Biophys. Chem. 59 (1996) 351–356.
[27] J. Juneja, J.B. Udgaonkar, Characterization of the unfolding of ribonuclease a by a pulsed hydrogen exchange study: evidence for competing pathways for unfolding, Biochemistry 41 (2002) 2641–2654.
[28] U. Arnold, A. Schierhorn, R. Ulbrich-Hofmann, Modification of the unfolding region in bovine pancreatic ribonuclease and its influence on the thermal stability and proteolytic fragmentation, Eur. J. Biochem. 259 (1999) 470–475.
[29] J. Köditz, R. Ulbrich-Hofmann, U. Arnold, Probing the unfolding region of ribonuclease A by site-directed mutagenesis, Eur. J. Biochem. 271 (2004) 4147–4156.
[30] U. Arnold, J. Köditz, Y. Markert, R. Ulbrich-Hofmann, Local fluctuations vs. global unfolding of proteins investigated by limited proteolysis, Biocatal. Biotransform. 23 (2005) 159–167.
[31] T.A. Klink, K.J. Woycechowsky, K.M. Taylor, R.T. Raines, Contribution of disulfide bonds to the conformational stability and catalytic activity of ribonuclease A, Eur. J. Biochem. 267 (2000) 566–572.
[32] J.H. Laity, S. Shimotakahara, H.A. Scheraga, Expression of wild-type and mutant bovine pancreatic ribonuclease A in *Escherichia coli*, Proc. Natl. Acad. Sci. U. S. A. 90 (1993) 615–619.
[33] P.S. Marfey, M. Uziel, J. Little, Reaction of bovine pancreatic ribonuclease a with 1,5-difluoro-2,4-dinitrobenzene. II. Structure of an intramolecularly bridged derivative, J. Biol. Chem. 240 (1965) 3270–3275.
[34] S.H. Lin, Y. Konishi, M.E. Denton, H.A. Scheraga, Influence of an extrinsic cross-link on the folding pathway of ribonuclease A. Conformational and thermodynamic analysis of cross-linked (lysine7-lysine41)-ribonuclease A, Biochemistry 23 (1984) 5504–5512.
[35] S.H. Lin, Y. Konishi, B.T. Nall, H.A. Scheraga, Influence of an extrinsic cross-link on the folding pathway of ribonuclease A. Kinetics of folding-unfolding, Biochemistry 24 (1985) 2680–2686.
[36] J. Futami, H. Tada, M. Seno, S. Ishikami, H. Yamada, Stabilization of human RNase 1 by introduction of a disulfide bond between residues 4 and 118, J. Biochem. 128 (2000) 245–250.
[37] T.A. Klink, R.T. Raines, Conformational stability is a determinant of ribonuclease A cytotoxicity, J. Biol. Chem. 275 (2000) 17463–17467.
[38] U. Arnold, C. Schulenburg, D. Schmidt, R. Ulbrich-Hofmann, Contribution of structural peculiarities of onconase to its high stability and folding kinetics, Biochemistry 45 (2006) 3580–3587.
[39] U. Arnold, C. Schulenburg, P. Pecher, R. Ulbrich-Hofmann, Impact of local structural regions on the protein stability as deduced from homologus, mutants, and mimics of RNase A, 7th International Conference on Protein Stabilisation, Exeter, UK, April 11th–14th, 2007.
[40] L. Pradeep, I. Kurinov, S.E. Ealick, H.A. Scheraga, Implementation of a k/k(0) method to identify long-range structure in transition states during conformational folding/unfolding of proteins, Structure 15 (2007) 1178–1189.
[41] Y. Markert, J. Köditz, R. Ulbrich-Hofmann, U. Arnold, Proline versus charge concept for protein stabilization against proteolytic attack, Protein Eng. 16 (2003) 1041–1046.
[42] F. Sanger, S. Nicklen, A.R. Coulson, DNA sequencing with chain-terminating inhibitors, Proc. Natl. Acad. Sci. U. S. A. 74 (1977) 5463–5467.
[43] C.N. Pace, F. Vajdos, L. Fee, G. Grimsley, T. Gray, How to measure and predict the molar absorption coefficient of a protein, Protein Sci. 4 (1995) 2411–2423.
[44] A. Tam, U. Arnold, M.B. Soellner, R.T. Raines, Protein prosthesis: 1,5-disubstituted [1,2,3]triazoles as cis-peptide bond surrogates, J. Am. Chem. Soc. 129 (2007) 12670–12671.
[45] C.N. Pace, E.J. Hebert, K.L. Shaw, D. Schell, V. Both, D. Krajcikova, J. Sevcik, K.S. Wilson, Z. Dauter, R.W. Hartley, G.R. Grimsley, Conformational stability and thermodynamics of folding of ribonucleases Sa, Sa2 and Sa3, J. Mol. Biol. 279 (1998) 271–286.
[46] U. Arnold, R. Ulbrich-Hofmann, Proteolytic degradation of ribonuclease A in the pretransition region of thermally and urea-induced unfolding, Eur. J. Biochem. 268 (2001) 93–97.
[47] U. Arnold, R. Ulbrich-Hofmann, Kinetic and thermodynamic thermal stabilities of ribonuclease A and ribonuclease B, Biochemistry 36 (1997) 2166–2172.
[48] U. Arnold, R. Ulbrich-Hofmann, Differences in the denaturation behavior of ribonuclease A induced by temperature and guanidine hydrochloride, J. Protein Chem. 19 (2000) 345–352.
[49] A.A. Frost, R.G. Pearson, Kinetik und Mechanismen homogener chemischer Reaktionen, Verlag Chemie, Weinheim, 1964.
[50] M.M. Santoro, D.W. Bolen, Unfolding free energy changes determined by the linear extrapolation method. 1. Unfolding of phenylmethanesulfonyl alpha-chymotrypsin using different denaturants, Biochemistry 27 (1988) 8063–8068.
[51] F. Leich, J. Köditz, R. Ulbrich-Hofman, U. Arnold, Tandemization endows bovine pancreatic ribonuclease with cytotoxic activity, J. Mol. Biol. 358 (2006) 1305–1313.
[52] K.L. Maxwell, D. Wildes, A. Zarrine-Afsar, M.A. De Los Rios, A.G. Brown, C.T. Friel, L. Hedberg, J.C. Horng, D. Bona, E.J. Miller, A. Vallee-Belisle, E.R. Main, F. Bemporad, L. Qiu, K. Teilum, N.D. Vu, A.M. Edwards, I. Ruczinski, F.M. Poulsen, B.B. Kragelund, S.W. Michnick, F. Chiti, Y. Bai, S.J. Hagen, L. Serrano, M. Oliveberg, D.P. Raleigh, P. Wittung-Stafshede, S.E. Radford, S.E. Jackson, T.R. Sosnick, S. Marqusee, A.R. Davidson, K.W. Plaxco, Protein folding: defining a "standard" set of experimental conditions and a preliminary kinetic data set of two-state proteins, Protein Sci. 14 (2005) 602–616.
[53] B. Hazes, B.W. Dijkstra, Model building of disulfide bonds in proteins with known three-dimensional structure, Protein Eng. 2 (1988) 119–125.
[54] J.L. Pellequer, S.W. Chen, Multi-template approach to modeling engineered disulfide bonds, Proteins 65 (2006) 192–202.
[55] K.J. Woycechowsky, K.D. Wittrup, R.T. Raines, A small-molecule catalyst of protein folding in vitro and in vivo, Chem. Biol. 6 (1999) 871–879.
[56] M. Matsumura, G. Signor, B.W. Matthews, Substantial increase of protein stability by multiple disulphide bonds, Nature 342 (1989) 291–293.
[57] F.M. Richards, P.J. Vithayathil, The preparation of subtilisn-modified ribonuclease and the separation of the peptide and protein components, J. Biol. Chem. 234 (1959) 1459–1465.
[58] E.E. Kim, R. Varadarajan, H.W. Wyckoff, F.M. Richards, Refinement of the crystal structure of ribonuclease S. Comparison with and between the various ribonuclease A structures, Biochemistry 31 (1992) 12304–12314.
[59] F.X. Schmid, H. Blaschek, A native-like intermediate on the ribonuclease A folding pathway. 2. Comparison of its properties to native ribonuclease A, Eur. J. Biochem. 114 (1981) 111–117.
[60] T. Kiefhaber, F.X. Schmid, Kinetic coupling between protein folding and prolyl isomerization. II. Folding of ribonuclease A and ribonuclease T1, J. Mol. Biol. 224 (1992) 231–240.
[61] F.X. Schmid, A native-like intermediate on the ribonuclease A folding pathway. 1. Detection by tyrosine fluorescence changes, Eur. J. Biochem. 114 (1981) 105–109.
[62] M. Iwaoka, W.J. Wedemeyer, H.A. Scheraga, Conformational unfolding studies of three-disulfide mutants of bovine pancreatic ribonuclease A and the coupling of proline isomerization to disulfide redox reactions, Biochemistry 38 (1999) 2805–2815.
[63] C.N. Pace, G.R. Grimsley, J.A. Thomson, B.J. Barnett, Conformational stability and activity of ribonuclease T1 with zero, one, and two intact disulfide bonds, J. Biol. Chem. 263 (1988) 11820–11825.
[64] S.F. Betz, Disulfide bonds and the stability of globular proteins, Protein Sci. 2 (1993) 1551–1558.
[65] J. Clarke, A.R. Fersht, Engineered disulfide bonds as probes of the folding pathway of barnase: increasing the stability of proteins against the rate of denaturation, Biochemistry 32 (1993) 4322–4329.
[66] J. Mansfeld, G. Vriend, B.W. Dijkstra, O.R. Veltman, B. Van den Burg, G. Venema, R. Ulbrich-Hofmann, V.G. Eijsink, Extreme stabilization of a thermolysin-like protease by an engineered disulfide bond, J. Biol. Chem. 272 (1997) 11152–11156.
[67] J.M. Mason, N. Gibbs, R.B. Sessions, A.R. Clarke, The influence of intramolecular bridges on the dynamics of a protein folding reaction, Biochemistry 41 (2002) 12093–12099.
[68] M.Y. Jeong, S. Kim, C.W. Yun, Y.J. Choi, S.G. Cho, Engineering a de novo internal disulfide bridge to improve the thermal stability of xylanase from *Bacillus stearothermophilus* No. 236, J. Biotechnol. 127 (2007) 300–309.
[69] C. Mitchinson, J.A. Wells, Protein engineering of disulfide bonds in subtilisin BPN', Biochemistry 28 (1989) 4807–4815.
[70] A.P. Hinck, D.M. Truckses, J.L. Markley, Engineered disulfide bonds in staphylococcal nuclease: effects on the stability and conformation of the folded protein, Biochemistry 35 (1996) 10328–10338.
[71] O.R. Siadat, A. Lougarre, L. Lamouroux, C. Ladurantie, D. Fournier, The effect of engineered disulfide bonds on the stability of *Drosophila melanogaster* acetylcholinesterase, BMC Biochem. 7 (2006) open access article No. 12.
[72] M. Mücke, F.X. Schmid, Intact disulfide bonds decelerate the folding of ribonuclease T1, J. Mol. Biol. 239 (1994) 713–725.